


Reexamining the framework for intermittency in Lagrangian stochastic models for turbulent flows: A way to an original and versatile numerical approach

Roxane Letournel*


*Laboratoire EM2C, CNRS, CentraleSupélec, Université Paris-Saclay, 3 rue Joliot Curie, 91192 Gif-sur-Yvette cedex, France;
Fédération de Mathématiques de CentraleSupélec, CNRS FR-3487, CentraleSupélec, Université Paris-Saclay, 9 rue Joliot Curie,
91190 Gif-sur-Yvette cedex, France;
and CMAP, CNRS, École Polytechnique, Institut Polytechnique de Paris, Route de Saclay, 91128 Palaiseau cedex, France*

Ludovic Goudenège 

*Fédération de Mathématiques de CentraleSupélec, CNRS FR-3487, CentraleSupélec, Université Paris-Saclay, 9 rue Joliot Curie,
91190 Gif-sur-Yvette cedex, France*

Rémi Zamansky 

Institut de Mécanique des Fluides de Toulouse (IMFT), Université de Toulouse, CNRS-INPT-UPS, Toulouse France

Aymeric Vié 

Laboratoire EM2C, CNRS, CentraleSupélec, Université Paris-Saclay, 3 rue Joliot Curie, 91192 Gif-sur-Yvette cedex, France

Marc Massot 

CMAP, CNRS, École Polytechnique, Institut Polytechnique de Paris, Route de Saclay, 91128 Palaiseau cedex, France



(Received 23 March 2021; accepted 27 May 2021; published 7 July 2021)

The characterization of intermittency in turbulence has its roots in the refined similarity hypotheses of Kolmogorov, and if no proper definition is to be found in the literature, statistical properties of intermittency were studied and models were developed in an attempt to reproduce it. The first contribution of this work is to propose a requirement list to be satisfied by models designed within the Lagrangian framework. Multifractal stochastic processes are a natural choice to retrieve multifractal properties of the dissipation. Among them, we investigate the Gaussian multiplicative chaos formalism, which requires the construction of a log-correlated stochastic process X_t . The fractional Gaussian noise of Hurst parameter $H = 0$ is of great interest because it leads to a log correlation for the logarithm of the process. Inspired by the approximation of fractional Brownian motion by an infinite weighted sum of correlated Ornstein-Uhlenbeck processes, our second contribution is to propose a stochastic model: $X_t = \int_0^\infty Y_t^x k(x) dx$, where Y_t^x is an Ornstein-Uhlenbeck process with speed of mean reversion x and k is a kernel. A regularization of $k(x)$ is required to ensure stationarity, finite variance, and logarithmic autocorrelation. A variety of regularizations are conceivable, and we show that they lead to the aforementioned multifractal models. To simulate the process, we eventually design a new approach relying on a limited number of modes for approximating the integral through a quadrature $X_t^N = \sum_{i=1}^N \omega_i Y_t^{x_i}$, using a conventional quadrature method. This method can retrieve the expected behavior with only one mode per decade, making this strategy versatile and computationally attractive for simulating such processes, while remaining within the proposed framework for a proper description of intermittency.

DOI: [10.1103/PhysRevE.104.015104](https://doi.org/10.1103/PhysRevE.104.015104)

I. INTRODUCTION

The stochastic nature of turbulence and the statistical behaviors of velocity fluctuations have been widely investigated, in order to understand and then reproduce its properties on reduced turbulence models (large eddy simulation) (see [1]). The inertial scales of many turbulent flows are correctly described by the classical image of Richardson's energy cascade

[2]. Kolmogorov formalized this universality of turbulence with a self-similar description of velocity fluctuations in the inertial range (see [3], hereafter referred to as K41). However, it was pointed out in Ref. [4] that this theory is flawed at small scales by the phenomenon of intermittent energy dissipation, in contradiction with the homogeneity assumed in K41.

Kolmogorov and Obukhov developed, in response to that concern, a vision based on local and scale-dependent observables which are more relevant to describe velocity fluctuations (see [5], hereafter referred to as K62). Since the publication of the refined similarity hypotheses, many studies have been devoted to data analysis, most of them focusing on energy

*roxane.letournel@centralesupelec.fr

dissipation. Consistently with these hypotheses, it was observed that the dissipation has a log-normal distribution and presents long-range power-law correlation (see Refs. [6–9]). Reproducing such behaviors in turbulence simulations is still an open problem and we are interested in the derivation of models that retrieve this intermittency in Reynolds averaged Navier-Stokes modelings or large eddy simulation (LES) contexts, in particular for modeling phenomena related to the small scales, such as combustion instabilities or the atomization of droplets in industrial burners.

Multifractal random fields are of primary interest for modeling intermittent fields since they possess high variability on a wide range of time or space scales, associated with intermittent fluctuations and long-range power-law correlations [10–12]. As opposed to monofractal, self-similar fields that correspond to the K41 description of turbulence, complex structures observed in Direct Numerical Simulation (DNS) and experimental studies are well reproduced by multifractal random fields.

The multiplicative cascade model of Yaglom [13] is at the basis of most cascade models introduced later to account for turbulent intermittency. It was able to reproduce both experimental facts and Kolmogorov’s log-normal hypothesis. Discrete models picture turbulence as an ensemble of discrete length scales, in which the energy transfers from a “mother” to a “daughter” eddy in a recursive and multiplicative manner. In this way, large fluctuations recursively generate correlations over long distances. Other discrete models were also formulated later and the reader is referred to the exhaustive review of [14]. However, in [15], Mandelbrot criticized these models for being based on a discrete and arbitrary ratio of length scales. They suggested to consider continuous models such as Gaussian multiplicative chaos, which was later formalized in Refs. [16,17]. The second criticism of [15] concerns the early cascade models that were developed in the Eulerian framework, and therefore do not exhibit a spatiotemporal structure, which was then introduced by means of stochastic causal models. The Lagrangian framework of intermittency was proposed in [10] and equivalent behavior of multifractal properties was observed for dissipation along particle trajectories. Causal and sequential multifractal stochastic processes were developed in response (see Refs. [18–22]). However, most of them rely on long-term memory stochastic processes and can be computationally expensive.

The first objective of this work is to establish a list of criteria for modeling intermittent dissipation. This characterization is based on observations of experimental data and is in accordance with the phenomenology developed by Kolmogorov. We show to what extent the Gaussian multiplicative chaos formalism is relevant for the proposed requirements.

Secondly, this work aims at developing a general framework for causal stochastic models based on Gaussian multiplicative chaos. In particular, the novelty lies in the construction of a log-correlated stochastic process X_t^∞ . Introducing the inverse Laplace transform of kernel functions of fractional Brownian motions, it is possible to express such stochastic processes by means of an infinite sum of Ornstein-Uhlenbeck processes. Such formulation is discussed and regularizations are proposed to ensure multifractal properties of the stochastic process X_t^∞ in the inertial range. We

eventually show that the newly introduced formulation encompasses most of the existing models.

Finally, we develop a numerical method for simulating this process, based on a quadrature of the infinite sum, i.e., on a finite sum of Ornstein-Uhlenbeck processes. This method is a discrete version of the process X_t^∞ and has the benefit of being computationally affordable and versatile. This discretization can be seen as the selection of representative timescales for the few Ornstein-Uhlenbeck processes all along the inertial range. The densification of these timescales corresponds to the continuous model X_t^∞ : with an infinity of timescales, each one is assigned to a turbulent structure and thus offers a natural physical interpretation.

Let us underline that stochastic calculus plays a crucial role in introducing and analyzing this modeling process as well as the asymptotic and singular limits. The purpose and scope of the present paper is related to the physical relevance of the introduced concepts and their impact in terms of numerical simulations of intermittent turbulent flows. Since the mathematical foundations of the results we use are out of the scope of this paper, we refer to a companion paper [23], where we propose a synthesis of the mathematical key results and their justification in terms of stochastic calculus.

The paper is organized as follows: In Sec. II we discuss the origins and the properties of intermittent dissipation for turbulent flows and we provide a characterization of it. We also recall the Gaussian multiplicative chaos formalism. Section III presents the procedure to express any fractional Brownian motion by an infinite sum of Ornstein-Uhlenbeck processes. Inspired by this formulation, we examine this new process and introduce necessary conditions to ensure its intermittency. We point out that this general formulation encompasses previous causal stochastic models. Then, in Sec. III, the numerical procedure to simulate the proposed stochastic process is described and we discuss the benefits and the physical grounds of such modeling.

II. PROPERTIES OF INTERMITTENCY IN TURBULENCE AND MULTIFRACTAL MODELS

A. Origins and properties of the intermittency

In Ref. [3], Kolmogorov first formalized the vision of Richardson cascade, “Big whirls have little whirls that feed on their velocity, and little whirls have lesser whirls and so on to viscosity,” by introducing the “Similarity hypothesis.” He stated that for high Reynolds numbers $\text{Re}_L = \frac{\sigma_u L}{\nu}$, where σ_u is the velocity standard deviation, L the characteristic length scale of fluid stirring, and ν the viscosity, turbulence is universal and velocity fluctuations statistics are expected to be independent of the large scales. Thus, the flow would be uniquely characterized by the viscosity and dissipation ε , defined by $\varepsilon = 2\nu S_{ij} S_{ij}$, with $S_{ij} = \frac{1}{2}(\frac{\partial u_i}{\partial x_j} + \frac{\partial u_j}{\partial x_i})$. Based on these two parameters, Kolmogorov scales can be introduced: $\eta \equiv (\nu^3/\langle\varepsilon\rangle)^{1/4}$, $u_\eta \equiv (\langle\varepsilon\rangle\nu)^{1/4}$, $\tau_\eta \equiv (\nu/\langle\varepsilon\rangle)^{1/2}$.

K41 states that in the inertial range, there is a complete similarity, and velocity increments statistics along Lagrangian trajectories are independent on viscosity and therefore only determined by the mean dissipation $\langle\varepsilon\rangle$ and the timescale τ :

$$[\Delta_\tau u]^2 = C_0(\varepsilon)\tau \quad \text{for } \tau_\eta \ll \tau \ll T_L, \quad (1)$$

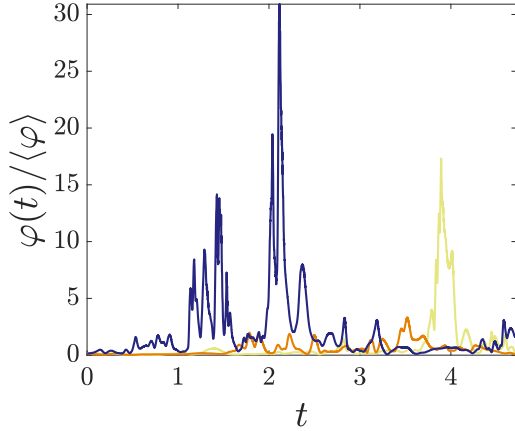


FIG. 1. Temporal evolution of the pseudodissipation along three particle trajectories obtained from the DNS dataset of [24].

where $\Delta_\tau u = u(t + \tau) - u(t)$ is the velocity increment along a fluid particle trajectory and C_0 the universal Lagrangian velocity structure function constant. The inertial range lies from the Kolmogorov timescale τ_η and the integral timescale $T_L = (1/\sigma_u^2) \int_0^\infty \langle u(t)u(t + \tau) \rangle d\tau$, which is the characteristic time of correlation of fluid particle velocity. Similar arguments with Eulerian velocity structure functions, defined with space increments, lead to the well-known theoretical “ $-5/3$ ” power law of the spatial energy spectrum.

The conservation of the rate of energy transfer in the inertial range, given by the Kolmogorov scaling $\langle \varepsilon \rangle \sim \frac{\sigma_u^2}{T_L} \sim \frac{\sigma_u^3}{L} \sim \frac{u_\eta^2}{\tau_\eta}$, allows us to obtain

$$\frac{L}{\eta} \sim \text{Re}_L^{3/4}, \quad \frac{T_L}{\tau_\eta} \sim \text{Re}_L^{1/2}. \quad (2)$$

However, there is some inconsistency in this theory [6,25,26]: C_0 was found not to be universal but Reynolds dependent. Furthermore this scaling could not be extended to higher order moments of the velocity increments because the instantaneous dissipation intermittently reaches very high values and so the global average of ε is not the relevant scale. This is illustrated in Fig. 1 where the pseudodissipation along fluid particle paths φ , an analogous variable to ε that we define later in Eq. (7), is plotted and exhibits brief and sudden high fluctuations. The long-range correlation of the dissipation indicates that the large scales of the flow influence the local dissipation rate, thus raising the question of the universality of the flow [27]. These remarks (raised in [4]) led Kolmogorov and Obukhov to the refined similarity hypothesis with the consideration of a locally averaged dissipation [5]. The subscript τ represents the timescale of the locally averaged variable.

$$\varepsilon_\tau(t) = \frac{1}{\tau} \int_t^{t+\tau} \varepsilon(s) ds. \quad (3)$$

The refined similarity hypothesis of K62 states that the statistics of velocity increments $\Delta_\tau u$ conditioned by local dissipation ε_τ is universal:

$$\langle [\Delta_\tau u]^p | \varepsilon_\tau \rangle = C_p \tau^{p/2} \varepsilon_\tau^{p/2}. \quad (4)$$

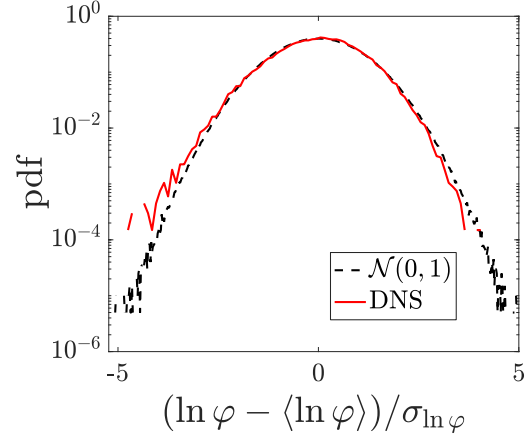


FIG. 2. Probability density function of the normalized variable $\ln \varphi$ compared to the Gaussian distribution (dashed black line). The y axis is on a logarithmic scale.

The unconditional statistics of the velocity increments therefore depend on the statistics of the locally averaged dissipation:

$$\langle [\Delta_\tau u]^p \rangle = C_p \tau^{p/2} \langle \varepsilon_\tau^{p/2} \rangle. \quad (5)$$

Such velocity structure functions have been studied and characterized in [28–31]. In K62, it was also suggested a log-normal distribution for ε_τ , with a logarithm scaling for the variance of $\ln \varepsilon_\tau$:

$$\sigma_{\ln \varepsilon_\tau}^2 \sim \ln \frac{T_L}{\tau}. \quad (6)$$

This prediction is in reasonable agreement with experimental data [32] and was also obtained in [13] with the discrete cascade model. These equations are not technically formulated in Kolmogorov’s theory, which is instead expressed in an Eulerian framework by spatially averaging ε . However, considering a time average along the trajectory of particles is a natural extension of K62 theory for Lagrangian increments and this formalism have already been adopted before [10,33,34].

The probability distribution function (PDF) of the pseudodissipation is in better agreement with the log-normal distribution than the classical dissipation, as shown in [7]. It is defined as

$$\varphi(\mathbf{x}, t) \equiv v \frac{\partial u_i}{\partial x_j} \frac{\partial u_i}{\partial x_j}. \quad (7)$$

As noted in [7], for homogeneous flows we have $\langle \varphi \rangle = \langle \varepsilon \rangle$. The Lagrangian variable is related to the Eulerian field by $\varphi(t) = \varphi(\mathbf{x}_f(t), t)$, where $\mathbf{x}_f(t)$ denotes the position of a fluid particle at time t . Figure 2 compares the PDF of $\ln \varphi$ obtained from the data of [24] with a normal distribution and we find good agreement. As suggested in K62 and measured in DNS by [35], we have $\sigma_{\ln \varphi}^2 = A + B \ln \text{Re}$.

The locally averaged dissipation (also called coarse-grained dissipation) can be defined by

$$\varphi_\tau(t) = \frac{1}{\tau} \int_t^{t+\tau} \varphi(s) ds. \quad (8)$$

This is the Lagrangian equivalent for the dissipation averaged over a ball of size ℓ considered by [5] in their refined similarity hypothesis. It is introduced in [10] to characterize multifractal properties for flow with large Reynolds numbers.

Numerous studies on data analysis of intermittency in turbulence reveal the multifractal nature of the pseudodissipation. The seminal work of Frisch [11] to characterize intermittency based on Kolmogorov theories was followed among others by [19,21,22,36–38]. Combining all the properties of intermittency mentioned in their work, we suggest the following list of criteria for the pseudodissipation to exhibit intermittency.

(1) Kolmogorov 1941 scaling: $\langle \varphi \rangle = \nu \tau_\eta^{-2}$.

(2) Kolmogorov 1962: φ is log-normal with $\sigma_{\ln \varphi}^2 \sim \ln \frac{T_L}{\tau_\eta}$.

(3) Multiscaling of the one-point statistics: $\langle \varphi^p \rangle \sim \left(\frac{T_L}{\tau_\eta}\right)^{\xi(p)}$, where $\xi(p)$ is a nonlinear function.

(4) Power-law scaling for the coarse-grained dissipation, in the inertial range: for $\tau_\eta \ll \tau \ll T_L$, $\langle \varphi_\tau^p \rangle \sim \left(\frac{T_L}{\tau}\right)^{\xi(p)}$. The last two points, II A and II A, are precisely the main characteristics of multifractal systems, which were considered for the modeling of the dissipation.

B. Modeling of the pseudodissipation

1. Multifractal models

In the Eulerian framework, discrete cascade models and later continuous random fields were developed. Yaglom proposed a model of multiplicative cascade where eddies can be seen as an ensemble of cells [13]. The largest scale is represented by a unique cell of size L and is then divided into smallest cells of size $\ell_1 = L/\lambda$ where λ is the constant scale ratio of the cascade model. This process is repeated until the smallest scales are reached, with the subdivision $\ell_N = \eta = L/\lambda^N$. The energy is transferred from one cell generation to the next with a positive ratio given by a random variable α_i with $\langle \alpha_i \rangle = 1$ that are independent and identically distributed. We can define for each cell of size ℓ_n the energy dissipation rate through it:

$$\varphi_{\ell_n} = \alpha_1 \alpha_2 \dots \alpha_n \langle \varphi \rangle. \quad (9)$$

Following the independence of the random variables α_i , it is straightforward to calculate the moments of any coarse-grained dissipation φ_{ℓ_n} :

$$\begin{aligned} \langle (\varphi_{\ell_n})^p \rangle &= \langle \varphi \rangle^p \prod_{i=1}^n \langle (\alpha_i)^p \rangle \\ &= \langle \varphi \rangle^p \langle \alpha_i^p \rangle^n \\ &= \langle \varphi \rangle^p \left(\frac{L}{\ell_n}\right)^{\xi(p)}, \end{aligned} \quad (10)$$

where we used $n = \ln_\lambda(L/\ell_n)$ and $\xi(p) = \ln_\lambda \langle \alpha_i^p \rangle$. Depending on the distribution of the α_i , different forms of $\xi(p)$ are found (see Refs. [39–41]). Such construction ensures immediately II A and II A, and $\varphi = \varphi_\eta = \alpha_1 \alpha_2 \dots \alpha_N \langle \varphi \rangle$ is log-normal according to the central limit theorem, assuming it applies.

Two main criticisms of these models are made in Ref. [15]. The first concerns the absence of spatiotemporal structure in these Eulerian representations of the dissipation fields which

lacks causality, a necessary ingredient. Equivalent Lagrangian models were then proposed, following the formalism of Lagrangian intermittency developed in [10]. The model of [18] is defined via a multiplicative process of independent stationary random processes with given correlation times. Properties II A and II A can here again only be verified for a finite number of scales depending on the constant scale ratio of the model λ .

This brings us to the second criticism raised in Ref. [15] which suggested to consider continuous cascade models such as Gaussian multiplicative chaos [16,17] for which no arbitrary scale is chosen. Stochastic integrals can be interpreted as an infinite sum, with continuous values of scales. Taking the exponential of stochastic integrals gives a “continuous product” instead of the discrete one defined in Eq. (9). Several models [19–22] are based on this formalism which allows one to combine the continuous vision of a cascade and a causal structure of the process. Specific properties of the stochastic integrals must be defined to ensure intermittency of the dissipation and we present them in the following section.

2. Gaussian multiplicative chaos

This section therefore reviews the Gaussian multiplicative chaos (GMC) formalism, introduced by Kahane [16], which allows one to build a process for the pseudodissipation $\varphi(t)$ and we show that it is in agreement with the criteria of intermittency defined in Sec. II A. The GMC involves the following form for the pseudodissipation:

$$\varphi(t) = \langle \varphi \rangle \exp(\chi_t), \quad (11)$$

where χ_t is a Gaussian process of variance σ_χ^2 . Its mean $\mu_\chi = -\frac{1}{2}\sigma_\chi^2$ is determined with the constraint that $\langle \exp(\chi_t) \rangle = 1$. We can parametrize this process by a zero-average Gaussian process X_t and the intermittency coefficient μ^ℓ :

$$\chi_t = \sqrt{\mu^\ell} X_t - \frac{\mu^\ell}{2} \sigma_X^2, \quad (12)$$

where μ^ℓ is given by $\mu^\ell = \sigma_\chi^2 / \sigma_X^2$ and the process X_t is constructed to be approximately log-correlated:

$$\langle X_t X_s \rangle \approx \ln_+ \frac{1}{|t-s|} + g(t, s), \quad (13)$$

where g is a bounded function and $\ln_+(u) = \max(\ln u, 0)$. The covariance kernel thus possesses a singularity and a standard approach consists in regularizing the distribution X_t by applying a “cut-off,” based on a small parameter τ_η such that, in the limit of $\tau_\eta \rightarrow 0$, $\varphi(t)$ is a GMC in a well-posed abstract framework. Further details and proof of convergence are derived in the complementary paper [23] which rigorously formalizes the construction of such a process as a limit of τ_η -regularized processes.

Let us show how the GMC is adapted to meet the intermittency criteria we have defined.

The mean value $\langle \varphi \rangle$ is chosen accordingly with requirement II A and the formalism of this model (i.e., exponential of a Gaussian variable) naturally ensures the log-normality of φ . Based on this formalism, it is possible to derive the moments of the dissipation and the coarse-grained dissipation

from the log-normal moments. Calculations are detailed in Appendix A. We obtain Eq. (A2) for the moments of the dissipation:

$$\langle \varphi^p \rangle = \langle \varphi \rangle^p \exp\left(\mu^\ell p(p-1) \frac{\sigma_X^2}{2}\right).$$

We can show that prescribing $\sigma_X^2 \sim \ln \frac{T_L}{\tau_\eta}$, which corresponds to the last part of requirement II A, readily ensures requirement II A:

$$\begin{aligned} \langle \varphi^p \rangle &\sim \langle \varphi \rangle^p \exp\left(\frac{\mu^\ell}{2} p(p-1) \ln \frac{T_L}{\tau_\eta}\right) \\ &\sim \left(\frac{T_L}{\tau_\eta}\right)^{\xi(p)} \end{aligned} \quad (14)$$

with the nonlinear scaling power law $\xi(p) = \frac{\mu^\ell}{2} p(p-1)$. This scaling is consistent with the large-scale dependency (related to the Reynolds number) of the pseudodissipation.

Finally, the multifractal property of the coarse-grained dissipation II A is ensured by the log-correlated autocorrelation of X_t . Indeed, prescribing $\langle X_t X_{t+\tau} \rangle \sim \ln \frac{T_L}{\tau}$ gives in Eq. (A4)

$$\begin{aligned} \langle \varphi_\tau^p \rangle &= \langle \varphi \rangle^p \int_{[0,1]^p} \exp\left(\mu^\ell \sum_{i<j} \langle X_{\tau s_i}, X_{\tau s_j} \rangle\right) \prod_{i=1}^p ds_i, \\ \frac{\langle \varphi_\tau^p \rangle}{\langle \varphi \rangle^p} &= \int_{[0,1]^p} \exp\left(\mu^\ell \sum_{i<j} \ln \frac{T_L}{\tau(s_j - s_i)}\right) \prod_{k=1}^p ds_k \\ &= \int_{[0,1]^p} \exp\left(\mu^\ell \frac{p(p-1)}{2} \ln \frac{T_L}{\tau} \right. \\ &\quad \left. - \mu^\ell \sum_{i<j} \ln(s_j - s_i)\right) \prod_{k=1}^p ds_k \\ &= \left(\frac{T_L}{\tau}\right)^{\xi(p)} \int_{[0,1]^p} \prod_{i<j} \frac{1}{(s_j - s_i)^{\mu^\ell}} \prod_{k=1}^p ds_k. \end{aligned} \quad (15)$$

Taking the limit $\text{Re} \rightarrow \infty$, the moments of φ diverge in Eq. (14) because φ is correlated over the large energy containing scales, whereas at a given scale τ , moments of φ_τ converge in Eq. (15), fulfilling the statistical properties required by the K62 phenomenology. It becomes independent of the Reynolds number and behaves as power law at small scales.

3. Illustration from DNS data

We illustrate this logarithmic behavior of the autocorrelation on DNS realizations available in [24]. Their simulations were run at $\tau_\eta = 0.02$. The integral Lagrangian time is found to be $T_L = 0.64$ which gives, according to Ref. [42], $\text{Re}_\lambda = (T_L/\tau_\eta)/0.08 = 400$. For each fluid particle, the process χ_t is obtained by taking the logarithm of the pseudodissipation along the particle trajectory. X_t^T is retrieved with the normalization of Eq. (12) and we plot in Fig. 3 its autocorrelation. One can easily verify by comparison with the logarithmic behavior in the dashed line that the autocorrelation follows a logarithmic behavior in the inertial range, i.e., between the τ_η and T_L of the simulation.

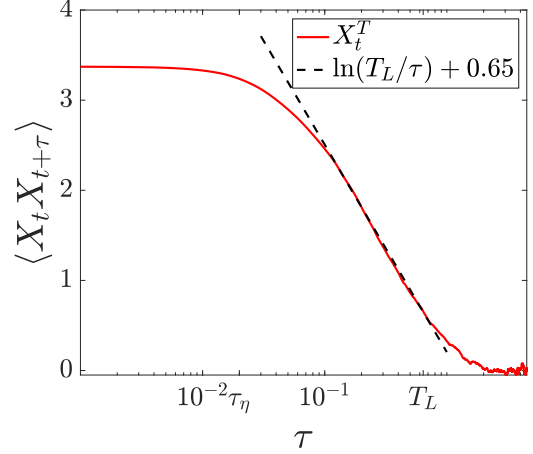


FIG. 3. Autocorrelation of X_t^T (red line) compared with expected logarithmic behavior (black dotted line). The x axis is on a logarithmic scale.

4. Conclusion

A characterization of the intermittency has been proposed in Sec. II A and we have checked that the proposed criteria are verified by a GMC modeling for the pseudodissipation. The remaining question to be addressed concerns the construction of the stochastic process X_t . Its variance must scale as the logarithm of the Reynolds number and its autocorrelation must be logarithmic in the inertial range. In the following, we summarize how such processes have been constructed in the literature.

C. Design of the X_t process

Pope originally suggested to represent φ as a log-normally correlated process by means of the Ornstein-Uhlenbeck process [7]. The stochastic equation they proposed for $\chi(t) = \ln[\varphi(t)/\langle \varphi \rangle]$ is the following:

$$d\chi_t = -\left(\chi_t + \frac{1}{2}\sigma_\chi^2\right) \frac{dt}{T_\chi} + \left(2\frac{\sigma_\chi^2}{T_\chi}\right)^{1/2} dW_t, \quad (16)$$

where W_t is a Wiener process, and T_χ is the integral timescale of χ , extracted from DNS and found to be close to the Lagrangian integral timescale T_L . The parameter σ_χ^2 is Reynolds number dependent and is also chosen accordingly to DNS data. The corresponding stochastic process X_t^{OU} in this case is driven by

$$dX_t^{\text{OU}} = -X_t^{\text{OU}} \frac{dt}{T_\chi} + \left(2\frac{\sigma_\chi^2}{T_\chi}\right)^{1/2} dW_t. \quad (17)$$

The autocorrelation of this process is well known and has an exponential decay in the form $\langle X_t X_{t+\tau} \rangle \sim e^{-\tau/T_\chi}$. It is plotted in blue in Fig. 4 and compared to the logarithmic behavior in the inertial range $[\tau_\eta, T_L] = [10^{-3}, 10^0]$. The exponential decay obviously does not reproduce the expected log-correlation of the autocorrelation. As a matter of fact, Pereira *et al.* showed in [22] that this model does not present the required multifractality for the coarse-grained process $\varphi_\tau(t)$.

Inspired by the stochastic process of Chevillard [21], they proposed to replace the Ornstein-Uhlenbeck process by a

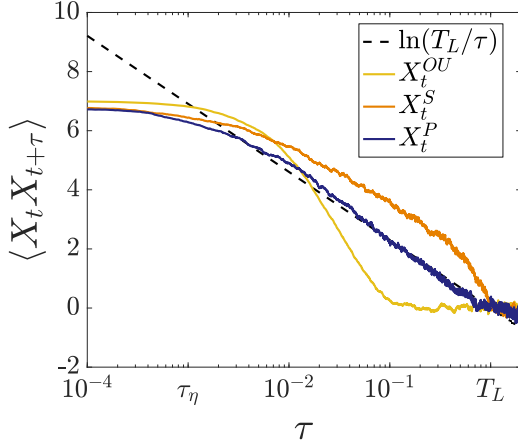


FIG. 4. Comparison of autocorrelation of processes of Pope and Chen [7] X_t^{OU} , Schmitt [38] X_t^S , and Pereira *et al.* [22] X_t^P with logarithmic behavior. Processes are rescaled for comparable variance of $\ln(T_L/\tau_\eta)$ and the x axis is on a logarithmic scale.

fractional Ornstein-Uhlenbeck process, which consists in replacing the Gaussian noise dW_t in the Langevin equation by a fractional Gaussian noise dW_t^H . Appropriate formalism for fractional Brownian motion (hereafter denoted fBm) was proposed in [43]. They defined the fBm of exponent H as a “moving average of dW_t , in which past increments of W_t , a Brownian motion, are weighted by the kernel $(t-s)^{H-1/2}$.” $H \in (0, 1)$ is called the Hurst parameter and defines the roughness of the path. Standard Brownian motion corresponds to $H = 1/2$ and is noted $W_t^{1/2} = W_t$. A classic expression for the Holmgren-Riemann-Liouville fractional Brownian motion is the following one:

$$W_t^H = \frac{1}{\Gamma(H + 1/2)} \int_0^t (t-s)^{H-1/2} dW_s. \quad (18)$$

The particular case of Hurst parameter $H = 0$ has a logarithmic autocorrelation [21], but as mentioned in Sec. II B 2, it is not well defined because of the singularity of its autocorrelation in 0. Mandelbrot [43] proposed a regularization of this fBm, for $\tau_\eta > 0$:

$$W_t^{\tau_\eta} = \frac{1}{\sqrt{\pi}} \int_0^t (t-s+\tau_\eta)^{-1/2} dW_s. \quad (19)$$

The calculation of its covariance gives, for any $t \geq s \geq 0$,

$$\begin{aligned} \langle W_t^{\tau_\eta} W_s^{\tau_\eta} \rangle &= \int_0^s (t-u+\tau_\eta)^{-1/2} (s-u+\tau_\eta)^{-1/2} du \\ &= \int_\tau^{s+\tau_\eta} \frac{1}{\sqrt{u} \sqrt{t-s+u}} du \\ &= [2 \ln(\sqrt{u} + \sqrt{u+t-s})]_{\tau_\eta}^{s+\tau_\eta} \\ &= 2 \ln \left(\frac{\sqrt{s+\tau_\eta} + \sqrt{t+\tau_\eta}}{\sqrt{\tau_\eta} + \sqrt{\tau + |t-s|}} \right). \end{aligned} \quad (20)$$

It is shown in [23] that the family of processes $\{W_t^\tau\}_{\tau>0}$ converges weakly in law to a Gaussian log-correlated process W_t^0 with covariance expressed in Eq. (13).

In their work, Schmitt and Marsan [19,38] developed the following causal stochastic process, inspired by this regular-

ized process:

$$X_t^S = \sqrt{\pi} (W_t^{\tau_\eta} - W_{t+\tau_\eta-T_L}^{\tau_\eta}) = \int_{t+\tau_\eta-T_L}^t (t-s+\tau_\eta)^{-1/2} dW_s \quad (21)$$

and showed its multifractal properties (scaling laws of the random process, of the coarse-grained process, logarithmic correlation of the logarithm of the process, etc.).

Pereira *et al.* [22], also used the increments of the regularized process in a fractional Ornstein-Uhlenbeck process to ensure stationarity of the process:

$$dX_t^P = -\frac{1}{T_L} X_t^P dt + \sqrt{\pi} dW_t^{\tau_\eta}. \quad (22)$$

Figure 4 compares the three processes described above with the logarithmic prediction of the autocorrelation in the inertial range ($[\tau_\eta, T_L] = [10^{-3}, 10^0]$). Both processes based on the fBm display long-range power-law correlation, as opposed to the Ornstein-Uhlenbeck process of Pope and Chen [7].

Subsequently, we will propose a stochastic model for X_t , also inspired by a regularized fBm. Beyond a purely mathematical construction of such a process, we would also like to introduce a natural physical interpretation before showing that it also allows a handy and efficient numerical implementation.

III. INFINITE SUM OF CORRELATED ORNSTEIN-UHLENBECK PROCESSES

We have seen that fBm presents interesting autocorrelation properties with long-range behavior. The objective of this section is to propose a formalism different from that of Eq. (18), which does not involve a moving average because its simulation would require large memory. The expression we derive in the following, however, relies on a combination of Ornstein-Uhlenbeck processes which are Markovian processes. This representation also makes it possible to make calculations (of moments and autocorrelation) easily, and to generate them by very simple calculation algorithms.

A. Approximation of fractional Brownian motion

The fractional Brownian motion as defined in Eq. (18) is a moving average and can be written in the following form:

$$B_t = \int_0^t K(t-s) dW_s. \quad (23)$$

Inspired by conventional techniques on linear time invariant systems, we introduce the “spectral” representation of the kernel K . This transformation is also proposed in Refs. [44,45].

$$K(u) = \int_0^\infty e^{-ux} k(x) dx, \quad (24)$$

where k is the inverse Laplace transform of K . If K satisfies certain measurability properties, stochastic Fubini theorem allows us to exchange the two integrals after replacing the

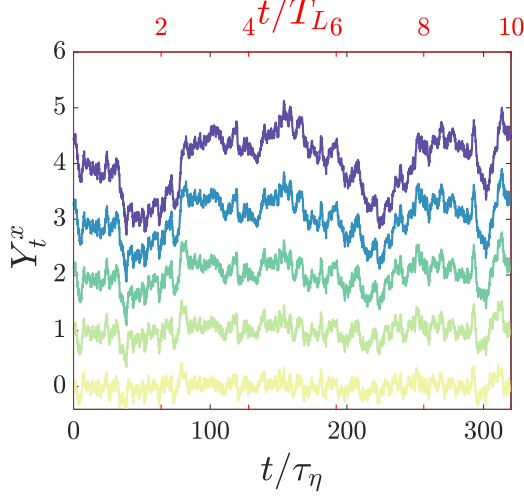


FIG. 5. Five correlated Ornstein-Uhlenbeck processes, driven by the same Wiener increments. Plots are shifted up for a better visualization and the color shades are darker with increasing characteristic times x^{-1} .

kernel by its spectral representation.

$$\begin{aligned}
 B_t &= \int_0^t K(t-s) dW_s \\
 &= \int_0^t \left(\int_0^\infty e^{-x(t-s)} k(x) dx \right) dW_s \\
 &= \int_0^\infty \left(\int_0^t e^{-x(t-s)} dW_s \right) k(x) dx \\
 &= \int_0^\infty \tilde{Y}_t^x k(x) dx, \tag{25}
 \end{aligned}$$

where $\tilde{Y}_t^x = \int_0^t e^{-x(t-s)} dW_s$ is a standardized Ornstein-Uhlenbeck process of parameter x and initial value $\tilde{Y}_0^x = 0$, solution of the stochastic differential equation:

$$d\tilde{Y}_t^x = -x\tilde{Y}_t^x dt + dW_t. \tag{26}$$

Let us insist on the fact that all the Ornstein-Uhlenbeck processes appearing in the integrand are driven by the same Wiener increments dW_t and are thus correlated to each other. Figure 5 shows five correlated processes \tilde{Y}_t^x with timescales ranging from $\tau_\eta = 0.02$ to $T_L = 0.64$. The process B_t is therefore a linear combination of standard Ornstein-Uhlenbeck processes, weighted by the kernel k .

We apply this technique to the fBm of Hurst parameter $H \in (0, 1)$ as defined in Eq. (18). The corresponding kernel is $K(t) = \Gamma(H + 1/2)^{-1} t^{H-1/2}$ and its inverse Laplace transform is $k(x) = \Gamma(H + 1/2)^{-1} \Gamma(-H - 1/2)^{-1} x^{-H-1/2}$. The fBm can finally be written

$$W_t^H = \frac{1}{\Gamma(H + 1/2)\Gamma(-H - 1/2)} \int_0^\infty \tilde{Y}_t^x x^{-H-1/2} dx, \tag{27}$$

and introducing the increments of the Ornstein-Uhlenbeck processes defined in Eq. (26), we readily obtain

$$dW_t^H \propto \int_0^\infty d\tilde{Y}_t^x x^{-H-1/2} dx. \tag{28}$$

We have shown that the fBm can be expressed as an infinite sum of correlated Ornstein-Uhlenbeck processes, weighted by k , the inverse Laplace transform of the initial kernel function K in the moving average of Eq. (18). This formulation has the advantage that no convolution product appears, and therefore the simulation of such a process does not require long-term memory. Inspired from this formalism, we propose an alternate process for X_t .

B. A stochastic process with appropriate regularizations

As shown in Sec. II C, fBm have been successfully used to reproduce multifractal properties and we therefore use the expression derived in Eq. (25) to suggest the following stochastic model for X_t :

$$X_t = \int_0^\infty Y_t^x k(x) dx, \tag{29}$$

where Y_t^x is an Ornstein-Uhlenbeck process of parameter x and $k(x)$ has to be determined. We now give the constraints on such model to ensure the stationarity, the finite variance, and the logarithmic autocorrelation of X_t .

1. Stationarity

A sufficient condition of stationarity for X_t is to impose stationarity for all the Ornstein-Uhlenbeck processes Y_t^x .

$$Y_t^x = \int_{-\infty}^t e^{-x(t-s)} dW_s. \tag{30}$$

2. Logarithmic autocorrelation

The autocorrelation of this process is

$$\begin{aligned}
 \langle X_t X_{t+\tau} \rangle &= \int_0^\infty \int_0^\infty \langle Y_t^x Y_{t+\tau}^y \rangle k(x) k(y) dx dy \\
 &= \int_0^\infty \int_0^\infty \frac{e^{-\tau y}}{x+y} k(x) k(y) dx dy, \tag{31}
 \end{aligned}$$

where the term $\langle Y_t^x Y_{t+\tau}^y \rangle$ is developed in Appendix B.

We have seen that a fBm of Hurst $H = 0$ has a logarithmic autocorrelation, at least approximately, i.e., apart from the singularity. Based on the inverse Laplace transformation of the kernel $K(t) \sim t^{-1/2}$, we propose $k(x) \sim x^{-1/2}$. However, this kernel possesses a singularity at 0 and we need to introduce regularizations to ensure a finite variance.

3. Finite variance

X_t is zero-averaged and its autocorrelation function only depends on the delay τ because of stationarity. The variance of the process can be expressed as

$$\int_0^\infty \int_0^\infty \frac{k(x)k(y)}{x+y} dx dy < \infty. \tag{32}$$

To satisfy and combine these three requirements, we propose to regularize the kernel k in the following way. One can see on the autocorrelation of Eq. (31) that any contribution of the function $k(y)$ for $y \gg 1/\tau$ will vanish because of the term $e^{-\tau y}$. Therefore, we introduce τ_η and we can assume $k(x) \sim x^{-1/2}$ only for $x \ll \tau_\eta^{-1}$, which is now compliant with

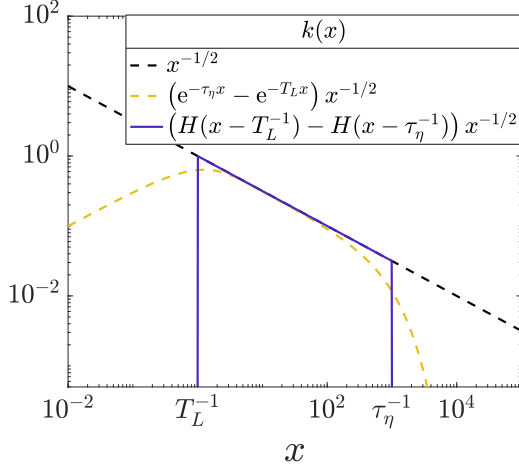


FIG. 6. Possible regularizations of the kernel $k(x)$ in a log-log scale.

the integrability on \mathbb{R}^+ . From a physical point of view, this regularization can be thought as a viscous cut-off.

A second regularization step is needed to ensure a finite variance of the process X_t , which corresponds to the need to introduce a large scale. More precisely, the second requirement II A specifies $\langle X_t^2 \rangle \sim \ln \frac{T_L}{\tau_\eta}$. It implies the integrability of $(x, y) \rightarrow \frac{k(x)k(y)}{x+y}$ on $(\mathbb{R}^+)^2$ and the logarithmic behavior in the inertial range is ensured by the requirement of $k(x) \sim x^{-1/2}$ for $T_L^{-1} \ll x \ll \tau_\eta^{-1}$.

In light of these regularizations, we propose a model for the process X_t^∞ . Note that we use the superscript “ ∞ ” because it highlights the use of an infinite sum of Ornstein-Uhlenbeck processes.

$$X_t^\infty = \int_0^\infty Y_t^x \frac{1}{\sqrt{\pi x}} [g_{T_L}(x) - g_{\tau_\eta}(x)] dx, \quad (33)$$

where g is such that the integral defined by the autocorrelation in Eq. (32) converges. A sufficient condition would be

$$g_\alpha(x) \rightarrow \begin{cases} 0 & \text{if } x \ll 1/\alpha \\ 1 & \text{if } x \gg 1/\alpha. \end{cases} \quad (34)$$

The calculations of the autocorrelation is given in Appendix C where we show that $\langle (X_t^\infty)^2 \rangle \sim \ln \frac{T_L}{\tau_\eta}$ and $\langle X_t^\infty X_{t+\tau}^\infty \rangle \sim \ln \frac{T_L}{\tau}$.

Examples of possible regularizations of the kernel $k(x) \sim x^{-1/2}$ are shown in Fig. 6: Cutting functions are $g_\alpha(x) = 1 - e^{-\alpha x}$ or $g_\alpha(x) = H(x - 1/\alpha)$ where H is the heaviside function.

The following section presents other types of regularizations in the spectral representation that can lead to existing processes.

C. A framework encompassing existing processes

In this section, we show that previous stochastic processes can be obtained from Eq. (29) with appropriate regularizations. The regularized fBm introduced in Ref. [43] in Eq. (19) can be expressed as an infinite sum of Ornstein-Uhlenbeck processes, introducing the inverse Laplace transform and applying Fubini’s theorem (as is done in Sec. III A).

The inverse Laplace transform of $K(t) = (t + \tau_\eta)^{-1/2}$ is $k_{\tau_\eta}(x) = e^{-\tau_\eta x} / \sqrt{\pi x}$. We obtain

$$W_t^{\tau_\eta} = \frac{1}{\sqrt{\pi}} \int_0^t (t - s + \tau_\eta)^{-1/2} dW_s = \frac{1}{\sqrt{\pi}} \int_0^\infty \tilde{Y}_t^x k_{\tau_\eta}(x) dx. \quad (35)$$

This exponential cutting function $e^{-\tau_\eta x}$ allows the process to be well defined, as opposed to the fBm of Hurst 0.

This process is now well defined, and with logarithmic autocorrelation, inherited from the behavior of the kernel in $x^{-1/2}$. However, it is not stationary and no large scales have been introduced: its variance is $\ln \frac{t + \tau_\eta}{\tau_\eta}$. This is why Pereira *et al.* [22] and Schmitt [38] introduced another regularization on the process.

Let us examine the process defined by Schmitt [38] and apply once again the same procedure as in Sec. III A:

$$\begin{aligned} X_t^S &= \int_{t+\tau_\eta-T_L}^t (t - s + \tau_\eta)^{-1/2} dW_s \\ &= \int_{t+\tau_\eta-T_L}^t \left(\int_0^\infty e^{-(t-s)x} k_{\tau_\eta}(x) dx \right) dW_s \\ &= \int_0^\infty \left(\int_{t+\tau_\eta-T_L}^t e^{-(t-s)x} dW_s \right) k_{\tau_\eta}(x) dx. \end{aligned} \quad (36)$$

To ensure finiteness of the variance, the Ornstein-Uhlenbeck processes must have a finite memory. In this case, the integral is truncated and the regularization consists in replacing the Ornstein-Uhlenbeck Y_t^x of Eq. (29), by $\int_{t-T_L+\tau_\eta}^t e^{-x(t-s)} dW_s$.

The process of Pereira *et al.* [22] is based on the increments of the regularized fBm: First, it is interesting to show that we can easily retrieve Chevillard’s expression of increments when applying the technique to the infinitesimal increment of $W_t^{\tau_\eta}$ [21]:

$$\begin{aligned} \sqrt{\pi} dW_t^{\tau_\eta} &= \int_0^\infty d\tilde{Y}_t^x k_{\tau_\eta}(x) dx \\ &= \int_0^\infty (-x \tilde{Y}_t^x dt + dW_t) k_{\tau_\eta}(x) dx \\ &= \int_0^\infty -x k_{\tau_\eta}(x) \int_0^t e^{-(t-s)x} dW_s dx dt \\ &\quad + \int_0^\infty k_{\tau_\eta}(x) dx dW_t. \end{aligned} \quad (37)$$

Using the Laplace transform for the first integral, we have $\mathcal{L}[x k_{\tau_\eta}(x)] = \mathcal{L}[\sqrt{x/\pi} e^{-\tau_\eta x}] = t^{-3/2}$. And the second integral is $\int_0^\infty k_{\tau_\eta}(x) dx = \tau_\eta^{-1/2}$. This yields

$$\begin{aligned} \sqrt{\pi} dW_t^{\tau_\eta} &= \int_0^t \frac{-1}{2} (t - s + \tau_\eta)^{-3/2} dW_s dt + \tau_\eta^{-1/2} dW_t \\ &= \tilde{\beta}_t^{\tau_\eta} dt + \tau_\eta^{-1/2} dW_t, \end{aligned} \quad (38)$$

TABLE I. Regularizations applied on the spectral representation of different processes. The logarithmic behavior of the autocorrelation of the process comes from the kernel behavior $x^{-1/2}$ in brown, its stationarity comes from the blue term, and the red terms ensure the finite variance.

Process	Definition	Spectral representation
fBm: $W_t^{\tau_\eta}$	$\frac{1}{\sqrt{\pi}} \int_0^t (t-s+\tau_\eta)^{-1/2} dW_s$	$\frac{1}{\sqrt{\pi}} \int_0^\infty \tilde{Y}_t^x \frac{e^{-\tau_\eta x}}{\sqrt{\pi x}} dx$
Schmitt: X_t^S	$\int_{t+\tau_\eta-T_L}^t (t-s+\tau_\eta)^{-1/2} dW_s$	$\int_0^\infty \left(\int_{t+\tau_\eta-T_L}^t e^{-(t-s)x} dW_s \right) \frac{e^{-\tau_\eta x}}{\sqrt{\pi x}} dx$
Pereira: X_t^P	$\sqrt{\pi} \int_{-\infty}^t e^{-(t-s)/T_L} dW_s^{\tau_\eta}$	$\int_0^\infty \left(\int_{-\infty}^t e^{-(t-s)/T_L} dY_s^x \right) \frac{e^{-\tau_\eta x}}{\sqrt{\pi x}} dx$
Pope: X_t^{OU}	$\int_{-\infty}^t \omega e^{-(t-s)/T_x} dW_s$	$\int_0^\infty Y_t^x \omega \delta(x - T_x^{-1}) dx$
X_t^∞	$\int_{-\infty}^t (t-s+\tau_\eta)^{-1/2} - (t-s+T_L)^{-1/2} dW_s$	$\int_0^\infty Y_t^x \frac{[g_{T_L}(x) - g_{\tau_\eta}(x)]}{\sqrt{\pi x}} dx$

where $\tilde{\beta}_t^{\tau_\eta} = \frac{-1}{2} \int_0^t (t-s+\tau_\eta)^{-3/2} dW_s$. In [22], they rather use the stationary version of this increment with $\beta_t^{\tau_\eta} = \frac{-1}{2} \int_{-\infty}^t (t-s+\tau_\eta)^{-3/2} dW_s$ and based on that increment, they regularize the process with

$$\begin{aligned} X_t^P &= \sqrt{\pi} \int_{-\infty}^t e^{-(t-s)/T_L} dW_s^{\tau_\eta} \\ &= \int_{-\infty}^t e^{-(t-s)/T_L} \int_0^\infty dY_s^x k_{\tau_\eta}(x) dx \\ &= \int_0^\infty \left(\int_{-\infty}^t e^{-(t-s)/T_L} dY_s^x \right) k_{\tau_\eta}(x) dx. \end{aligned} \quad (39)$$

Therefore, the regularization for stationarity consists in replacing the Ornstein-Uhlenbeck Y_t^x of Eq. (29), by $\int_{-\infty}^t e^{-(t-s)/T_L} dY_s^x$.

Finally, we can see that taking a Dirac function for $k(x)$ corresponds to Pope and Chen's process [7]:

$$X_t^{\text{OU}} = \int_{-\infty}^t \omega e^{-(t-s)/T_x} dW_s = \int_0^\infty Y_t^x \omega \delta(x - T_x^{-1}) dx, \quad (40)$$

where $\omega = (2\frac{\sigma_x^2}{T_x})^{1/2}$ is the scaling factor in front of the Gaussian noise in Eq. (16). This kernel representation does not exhibit a behavior in $x^{-1/2}$, and we already know that the single Ornstein-Uhlenbeck process is not log-correlated.

Table I summarizes the different regularizations for all these processes. It shows that the general formalism of Eq. (29) is a framework that encompasses existing processes depending on the three criteria for the regularization.

If the general formalism proposed in Eq. (29) gives the possibility to represent and simulate these processes using Ornstein-Uhlenbeck processes, one can see that their simulation is not equivalent. The processes of Schmitt [38] and Pereira *et al.* [22] require one to keep in memory the history of the process since at each instant t , the set of realizations of W_s and Y_s^x , respectively, for s in the intervals $[t+\tau_\eta-T_L, t]$ and $]-\infty, t]$, respectively, should be involved in the computation (it is actually truncated for the numerical simulation). It is not the case for the one we propose in Eq. (33) and we develop in the following section a numerical approach to implement such process with no long-term memory.

IV. FINITE SUM OF CORRELATED ORNSTEIN-UHLENBECK PROCESSES

A. Quadrature

Following the idea of [45], with an appropriate quadrature, the integral can be replaced by a system of finite number of Ornstein-Uhlenbeck processes. We call X_t^∞ the process defined with the infinite sum and X_t^N the one obtained with N points of quadrature.

$$X_t^\infty \equiv \int_0^\infty Y_t^x \frac{1}{\sqrt{\pi x}} [g_{T_L}(x) - g_{\tau_\eta}(x)] dx \approx X_t^N \equiv \sum_{i=1}^N \omega_i Y_t^{x_i}. \quad (41)$$

Because of the regularizing functions $g_{T_L} - g_{\tau_\eta}$, it is useless to compute quadrature points far outside the inertial range $[T_L^{-1}; \tau_\eta^{-1}]$. For simplicity, we use in the following examples Heaviside functions for g . Considering the logarithmic shape of the kernel, we propose a geometric partition of this domain, along with a middle-Riemann sum for the weights:

$$\text{for } i = 1, \dots, N \begin{cases} x_i &= \frac{1}{T_L} \left(\frac{T_L}{\tau_\eta} \right)^{(i-1/2)/N}, \\ \omega_i &= \frac{1}{\sqrt{\pi x_i}} \Delta x_i, \end{cases} \quad (42)$$

where $\Delta x_i = \frac{1}{T_L} \left(\frac{T_L}{\tau_\eta} \right)^{i/N} - \frac{1}{T_L} \left(\frac{T_L}{\tau_\eta} \right)^{(i-1)/N}$. Figure 7 shows the kernel approximation with $N = 10$ points of quadrature. The kernel $x^{-1/2}$ is approached by step functions all along the inertial range. The weights can be normalized to match the variance of the analytic process $\langle (X_t^\infty)^2 \rangle$. The normalizing factor R is given by

$$R = \frac{\sigma_{X_t^\infty}}{\sigma_{X_t^N}} = \sqrt{\langle (X_t^\infty)^2 \rangle} \left(\sum_{i,j} \frac{\omega_i \omega_j}{x_i + x_j} \right)^{-1/2}. \quad (43)$$

Figure 8 shows the autocorrelation of the process X_t^∞ compared with the discrete one X_t^N . As demonstrated in Appendix C, it is clear that the infinite sum has indeed a logarithmic autocorrelation; it follows the dashed line all along the inertial range. A one-point quadrature, corresponding to a single Ornstein-Uhlenbeck process, is plotted in the lightest yellow in the figure. As discussed above, this specific process corresponds to $X_t^1 = X_t^{\text{OU}}$ and does not have a logarithmic autocorrelation all along the inertial range. With two points of quadrature, the autocorrelation displays two bumps, around

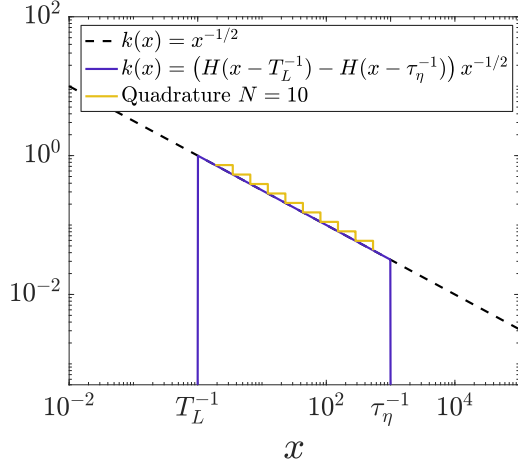


FIG. 7. The kernel behavior $k(x) \sim x^{-1/2}$ in the dashed line is regularized with Heaviside cutting functions in dark blue and compared to its quadrature representation in light yellow. The x and y scales are logarithmic.

the two timescales of the Ornstein-Uhlenbeck processes. The autocorrelation range has been extended but it is not yet clear that it follows a logarithmic behavior. With more quadrature points (darker lines), the autocorrelation of X_t^N is getting closer to the analytical one.

This convergence of the autocorrelation can be explicit introducing the relative difference between the analytical autocorrelation $\rho^\infty(\tau)$ and the one obtained from the quadrature $\rho^N(\tau)$:

$$\begin{aligned} \rho^\infty(\tau) &\equiv \int_{T_L^{-1}}^{\tau_\eta^{-1}} \int_{T_L^{-1}}^{\tau_\eta^{-1}} f(\tau, x, y) dx dy, \\ \rho^N(\tau) &\equiv \sum_{i=1}^N \sum_{j=1}^N f(\tau, x_i, x_j) \Delta x_i \Delta x_j, \end{aligned} \quad (44)$$

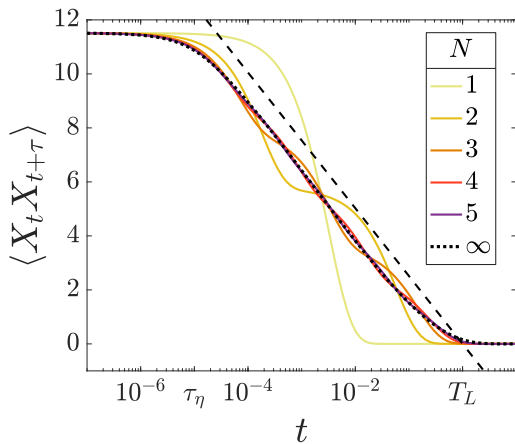


FIG. 8. Comparison of the autocorrelations of the analytical process (dotted black line) and the discrete one for a finite number of modes. The inertial range covers 5 decades. The x axis is on a logarithmic scale and the dashed line represents the expected logarithmic behavior.

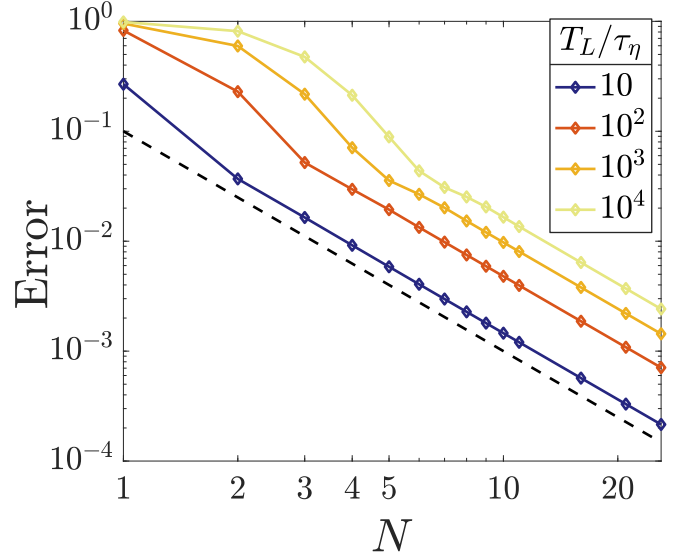


FIG. 9. Error in log-log scale between the L_2 norm of the discrete process X_t^N and the analytical process X_t^∞ . The dashed line represents a slope of -2 .

where $f(\tau, x, y) = \frac{e^{-\tau y}}{(x+y)\sqrt{xy}}$. The numerical convergence is verified in Fig. 9 with the error defined as

$$\text{Error} = \sqrt{\int_{\tau_\eta}^{T_L} \left(\frac{\rho^\infty(\tau) - \rho^N(\tau)}{\rho^\infty(\tau)} \right)^2 d\tau}. \quad (45)$$

As observed in Fig. 9, the order of convergence is 2. The value of the error is shifted when increasing the inertial range. With one Ornstein-Uhlenbeck per decade, the relative error is below 10%. We can therefore postulate that an acceptable number of processes would be one or two per decade. Figure 10 illustrates this choice, with different inertial ranges. The number of points for the discrete process is chosen accordingly and we verify the logarithmic behavior of such processes all along the inertial range. For instance, with an inertial range covering

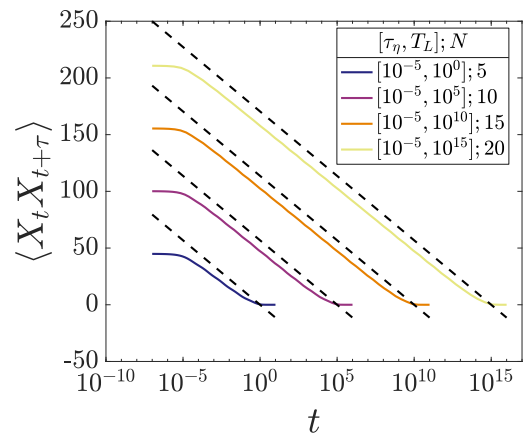


FIG. 10. Autocorrelation of X_t for different inertial ranges in log-log scale, compared with logarithmic behavior in dashed lines. The number of points chosen in the quadrature N corresponds to the number of decades covered by the inertial range $[\tau_\eta, T_L]$.

20 decades (upper yellow line in Fig. 10), that corresponds to $\text{Re}_\lambda \sim 10^{11}$, only 20 Ornstein-Uhlenbeck processes are needed to approach a logarithmic behavior of the autocorrelation all along the inertial range.

B. Discussion

A new log-correlated process X_t^∞ and its discrete version with N Ornstein-Uhlenbeck processes X_t^N have been presented. In this section, we will discuss their physical interpretation and their advantage over existing processes.

1. Physical interpretation

X_t^N can be seen as an extension of Pope and Chen's process [7]. We recall that the latter corresponds to $N = 1$ with quadrature points taken as

$$x_1 = \frac{1}{T_\chi} \quad \text{and} \quad \omega_1 = \sqrt{\frac{2\sigma_\chi^2}{\mu^\ell T_\chi}}. \quad (46)$$

[7] observed that T_χ scales with the integral timescale T_L and σ_χ scales with the logarithm of Reynolds number. By comparison with our proposition of quadrature, we would suggest to use $T_\chi = \sqrt{T_L \tau_\eta}$, and σ_χ is indeed scaling as $\sigma_\chi \sim \ln \frac{T_L}{\tau_\eta}$ to ensure requirement II A.

For Reynolds number $\text{Re}_\lambda \sim \frac{T_L}{0.08\tau_\eta} \approx 125$, we have seen that a single Ornstein-Uhlenbeck is enough to cover the entire inertial range and the exponential decay mimics the logarithmic behavior in such small interval. However, for larger Reynolds number, it is necessary to extend the long range of the autocorrelation by adding other Ornstein-Uhlenbeck processes, evenly distributed all along the inertial range. A perfect logarithmic scaling is retrieved with an infinity of Ornstein-Uhlenbeck processes.

This new process also makes a very simple link between “continuous” processes with no timescale (or here, an infinity), corresponding to X_t^∞ and “discrete” cascade models X_t^N , where arbitrary timescales are chosen to each represent a turbulent structure. A turbulent cascade is often represented as a product of independent processes defined at each scale, each one presenting a characteristic timescale. The approximation of X_t^∞ by X_t^N exactly consists in selecting representative timescales, and the coherence of the whole cascade is ensured by the fact that every Ornstein-Uhlenbeck process is correlated to each other because they are driven by the exact same Gaussian noise.

2. Implementation

Unlike the models of [22,38], the process has no “self-memory.” It is the combination of several Ornstein-Uhlenbeck processes, with adapted characteristic timescales that can mimic this long-range correlation. The closer the characteristic times of the Ornstein-Uhlenbeck processes, the better the logarithmic approximation (quadrature with a large number of points), but we show that one timescale per decade is already enough to retrieve the approximate long-range behavior. This considerably reduces the computational cost of the simulation of such process. Simulating Ornstein-Uhlenbeck processes is very common, rapid, and does not require one to keep a

memory of the history of the path, as opposed to the convolution form used in Refs. [22,38].

3. A causal multifractal process for pseudodissipation

An analytical stochastic equation can be derived for the pseudodissipation, which is the variable of interest used in Lagrangian stochastic models. First, we can retrieve an analogous formulation for the increments of X_t^∞ , introducing the β function already used in [22].

$$\begin{aligned} dX_t^\infty &= \int_0^\infty dY_t^x \frac{e^{-x\tau_\eta} - e^{-xT_L}}{\sqrt{\pi x}} dx \\ &= \int_0^\infty (-xY_t^x dt + dW_t) \frac{e^{-x\tau_\eta} - e^{-xT_L}}{\sqrt{\pi x}} dx \\ &= \frac{-1}{2} \int_{-\infty}^t ((t-s+\tau_\eta)^{-3/2} - (t-s+T_L)^{-3/2}) dW_s dt \\ &\quad + \left(\frac{1}{\sqrt{\tau_\eta}} - \frac{1}{\sqrt{T_L}} \right) dW_t \\ &= (\beta_t^{\tau_\eta} - \beta_t^{T_L}) dt + \left(\frac{1}{\sqrt{\tau_\eta}} - \frac{1}{\sqrt{T_L}} \right) dW_t. \end{aligned} \quad (47)$$

We recall that the Lagrangian multiplicative chaos, which is causal and stationary, is readily obtained while exponentiating the Gaussian process X_t^∞ : $\varphi = \langle \varphi \rangle \exp(\sqrt{\mu^\ell} X_t^\infty - \frac{\mu^\ell \sigma_\chi^2}{2})$. Application of Ito's lemma gives the Lagrangian stochastic dynamics of the pseudodissipation, namely,

$$\begin{aligned} \frac{d\varphi}{\varphi} &= \left[\sqrt{\mu^\ell} (\beta_t^{\tau_\eta} - \beta_t^{T_L}) + \frac{\mu^\ell}{2} \left(\frac{1}{\sqrt{\tau_\eta}} - \frac{1}{\sqrt{T_L}} \right)^2 \right] dt \\ &\quad + \sqrt{\mu^\ell} \left(\frac{1}{\sqrt{\tau_\eta}} - \frac{1}{\sqrt{T_L}} \right) dW_t. \end{aligned} \quad (48)$$

Of course, the implementation of this stochastic equation preferentially uses the expression of β in the Laplace domain and we recall that the same Wiener process is used in the N Ornstein-Uhlenbeck processes $Y_t^{x_i}$ but also in dW_t in Eq. (48). Numerically, we replace the β functions by its quadrature:

$$\begin{aligned} \beta_t^{\tau_\eta} - \beta_t^{T_L} &= \int_0^\infty -xY_t^x \frac{g_{T_L}(x) - g_{\tau_\eta}(x)}{\sqrt{\pi x}} dx \\ &\approx \sum_{i=1}^N -x_i \omega_i Y_t^{x_i}. \end{aligned} \quad (49)$$

V. CONCLUSION

Intermittency in turbulence can be characterized by multifractal properties of the dissipation. A Gaussian multiplicative chaos formalism allows us to model such dissipation process, but relies on the introduction of a zero-average Gaussian and log-correlated process, X_t . In the literature, such processes were defined based on a regularized fBm; they lack physical interpretation and can be computationally expensive in simulations.

In this contribution, we have introduced another way to build such processes, with a general form [Eq. (29)] that requires regularizations. We have shown that specific regularizations yield existing processes, and we propose

an alternate one, which has the benefits of relying on an infinite combination of Ornstein-Uhlenbeck processes. Characteristic timescales of those Ornstein-Uhlenbeck processes are covering the inertial range, between Kolmogorov timescale and the integral timescale. Each of them represents a specific turbulence structure; this corresponds to a continuous cascade model where no arbitrary timescale is needed.

We have presented only essential ingredients of stochastic calculus for the purpose of presenting the framework from a physical perspective but the details of the mathematical foundations can be found in a companion paper [23]. A discrete version of this process is proposed, based on a selection of a few specific modes, corresponding to representative characteristic timescales. The quadrature of the infinite sum is therefore a finite sum of Ornstein-Uhlenbeck processes, logarithmically distributed in the inertial range. This corresponds to a discrete cascade model.

Besides the simplicity of simulation, this model has the benefit to be very adaptable and can be envisioned to be useful for future perspectives: dissipation along the trajectory of solid inertial particles is not logarithmic anymore but the model can actually fit any autocorrelation function.

Thanks to the versatility of the process, application to LES can also be considered, with different regularizing functions, where the cut-off could be based on the subgrid timescale, for instance.

ACKNOWLEDGMENTS

This work was supported by grants from Region Ile-de-France DIM MATHINNOV. Support from the French Agence Nationale de la Recherche through the MIMETYC project (Grant No. ANR-17-CE22-0003) is also acknowledged.

APPENDIX A: MOMENTS OF THE DISSIPATION AND COARSE-GRAINED DISSIPATION

The GMC formalism gives $\varphi(t) = \langle \varphi \rangle \exp(\chi_t)$, with $\chi_t = \sqrt{\mu^\ell} X_t - \frac{\mu^\ell}{2} \langle X_t^2 \rangle$. It is immediate that the variance of χ_t can be expressed with the variance of X_t : $\sigma_\chi^2 = \mu^\ell \sigma_X^2$.

χ_t is a Gaussian variable, with moments generating function equal to

$$M_\chi(p) = \langle \exp(p\chi_t) \rangle = \exp\left(p\mu_\chi + \frac{1}{2}p^2\sigma_\chi^2\right) \quad (\text{A1})$$

Using $\mu_\chi = -\frac{1}{2}\sigma_\chi^2$, this simplifies to

$$\langle \varphi^p \rangle = \langle \varphi \rangle^p \exp\left(p(p-1)\frac{\sigma_\chi^2}{2}\right). \quad (\text{A2})$$

Moments of the coarse-grained dissipation can also be derived as a function of the autocorrelation of X_t :

$$\begin{aligned} \langle \varphi_\tau \rangle^p &= \frac{1}{\tau^p} \int_{[t, t+\tau]^p} \prod_{i=1}^p \varphi(s_i) ds_i \\ &= \frac{\langle \varphi \rangle^p}{\tau^p} \int_{[t, t+\tau]^p} \exp\left(\sum_{i=1}^p \sqrt{\mu^\ell} X_{s_i} - p\frac{\mu^\ell}{2} \sigma_X^2\right) \prod_{i=1}^p ds_i. \end{aligned} \quad (\text{A3})$$

Using the well-known identity $\langle \exp(g) \rangle = \exp\left(\frac{\langle g^2 \rangle}{2}\right)$ for any zero-average Gaussian variable g , we have

$$\begin{aligned} \langle \varphi_\tau \rangle^p &= \frac{\langle \varphi \rangle^p}{\tau^p} e^{-p(\mu^\ell/2)\sigma_X^2} \int_{[t, t+\tau]^p} \exp\left(\frac{1}{2} \sum_{i,j=1}^p \mu^\ell \langle X_{s_i} X_{s_j} \rangle\right) \prod_{i=1}^p ds_i \\ &= \frac{\langle \varphi \rangle^p}{\tau^p} e^{-p(\mu^\ell/2)\sigma_X^2} \int_{[t, t+\tau]^p} \exp\left(\sum_{i<j} \mu^\ell \langle X_{s_i} X_{s_j} \rangle + p\frac{\mu^\ell}{2} \sigma_X^2\right) \prod_{i=1}^p ds_i \\ &= \langle \varphi \rangle^p \int_{[0,1]^p} \exp\left(\mu^\ell \sum_{i<j} \langle X_{\tau s_i} X_{\tau s_j} \rangle\right) \prod_{i=1}^p ds_i. \end{aligned} \quad (\text{A4})$$

The last line results from a change of variables and the stationarity of the processes.

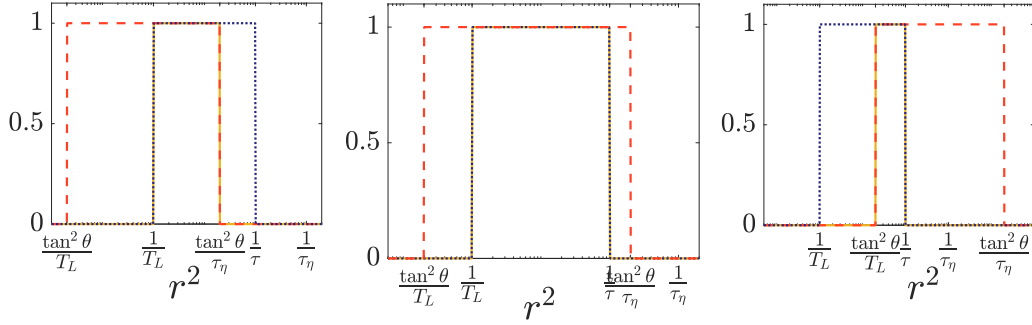


FIG. 11. The yellow line represents the functions B (on the left), C (in the middle), and D (on the right) plotted for three examples of θ . The dotted blue line is $[g_\tau(r^2) - g_{T_L}(r^2)]$ and the dashed red line is $[g_{\tau_\eta/\tan^2\theta}(r^2) - g_{T_L/\tan^2\theta}(r^2)]$.

APPENDIX B: TWO-POINTS CORRELATION OF ORNSTEIN-UHLENBECK CORRELATED PROCESSES

Let us write $Y_t^x = \int_{-\infty}^t e^{-(t-x)s} dW_s$. For any $x_i, x_j \in [0, +\infty[$ and $t > 0$ and $\tau > 0$, we have

$$\begin{aligned} \langle Y_t^{x_i} Y_{t+\tau}^{x_j} \rangle &= \left\langle \int_{-\infty}^t e^{-x_i(t-s)} dW_s \int_{-\infty}^{t+\tau} e^{-x_j(t+\tau-s)} dW_s \right\rangle \\ &= e^{-(x_i+x_j)t} e^{-x_j\tau} \int_{-\infty}^t e^{(x_i+x_j)s} ds \\ &= \frac{e^{-x_j\tau}}{x_i + x_j}. \end{aligned} \quad (\text{B1})$$

APPENDIX C: VARIANCE AND AUTOCORRELATION OF X_t^∞

We calculate the autocorrelation of the process

$$X_t^\infty = \int_0^\infty Y_t^x \frac{1}{\sqrt{\pi x}} [g_{T_L}(x) - g_{\tau_\eta}(x)] dx. \quad (\text{C1})$$

We denote $I = \langle X_t^\infty X_{t+\tau}^\infty \rangle$. We can consider, without loss of generality, $e^{-\tau y} = 1 - g_\tau(y)$.

$$\begin{aligned} I &= \frac{1}{\pi} \int_0^\infty \int_0^\infty \frac{e^{-\tau y}}{(x+y)\sqrt{xy}} [g_{T_L}(x) - g_{\tau_\eta}(x)] [g_{T_L}(y) - g_{\tau_\eta}(y)] dx dy \\ &= \frac{1}{\pi} \int_0^\infty \int_0^\infty \frac{1}{(x+y)\sqrt{xy}} [g_{T_L}(x) - g_{\tau_\eta}(x)] [g_{T_L}(y) - g_\tau(y)] dx dy \\ &= \frac{4}{\pi} \int_0^{\pi/2} \int_{r=0}^\infty \frac{[g_\tau(r^2) - g_{T_L}(r^2)] [g_{\tau_\eta/\tan^2\theta}(r^2) - g_{T_L/\tan^2\theta}(r^2)]}{r} dr d\theta \end{aligned} \quad (\text{C2})$$

by using the transformation $(x, y) = (r^2 \cos^2 \theta, r^2 \sin^2 \theta)$ whose Jacobian is

$$-2r \cos(\theta)^2 2r^2 \cos(\theta) \sin(\theta) - 2r^2 \cos(\theta) \sin(\theta) 2r \sin(\theta)^2 = -4r^3 \cos(\theta) \sin(\theta). \quad (\text{C3})$$

The integral I can be split into five parts according to the value of θ . We introduce the functions A, B, C, D, E all defined by the product $[g_\tau(r^2) - g_{T_L}(r^2)] [g_{\tau_\eta/\tan^2\theta}(r^2) - g_{T_L/\tan^2\theta}(r^2)]$ but for different ranges of θ .

$$\begin{aligned} I\pi/4 &= \int_0^{\tan^{-1} \sqrt{\tau_\eta/T_L}} \int_{r=0}^\infty \frac{A(r^2)}{r} dr d\theta + \int_{\tan^{-1} \sqrt{\tau_\eta/T_L}}^{\tan^{-1} \sqrt{\tau_\eta/\tau}} \int_{r=0}^\infty \frac{B(r^2)}{r} dr d\theta \\ &+ \int_{\tan^{-1} \sqrt{\tau_\eta/\tau}}^{\pi/4} \int_{r=0}^\infty \frac{C(r^2)}{r} dr d\theta + \int_{\pi/4}^{\tan^{-1} \sqrt{T_L/\tau}} \int_{r=0}^\infty \frac{D(r^2)}{r} dr d\theta \\ &+ \int_{\tan^{-1} \sqrt{T_L/\tau}}^{\pi/2} \int_{r=0}^\infty \frac{E(r^2)}{r} dr d\theta. \end{aligned} \quad (\text{C4})$$

To help the reader visualize the products of the regularized g functions, we show in Fig. 11 the schemes for the resulting product of the g functions. The first and last integrals are equal to zero because the ‘‘door’’ functions do not have any

superposition. We can see from Fig. 11 that B , C , and D simplify to

$$\begin{aligned} B(r^2) &= g_{T_L}(r^2) - g_{\tau_\eta/\tan^2\theta}(r^2), \\ C(r^2) &= g_{T_L}(r^2) - g_\tau(r^2), \\ D(r^2) &= g_{T_L/\tan^2\theta}(r^2) - g_\tau(r^2). \end{aligned} \quad (\text{C5})$$

We use the property of the regularizing functions g_α :

$$\begin{aligned} \int_0^\infty \frac{g_{\tau_1}(r^2) - g_{\tau_2}(r^2)}{r} dr &\approx \int_{\sqrt{\tau_1^{-1}}}^{\sqrt{\tau_2^{-1}}} \frac{1}{r} dr = \frac{1}{2} \ln \frac{\tau_1}{\tau_2}, \\ I\pi/4 &= \int_{\tan^{-1}\sqrt{\tau_\eta/T_L}}^{\tan^{-1}\sqrt{\tau_\eta/\tau}} \frac{1}{2} \ln\left(\frac{T_L \tan^2\theta}{\tau_\eta}\right) d\theta + \int_{\tan^{-1}\sqrt{\tau_\eta/\tau}}^{\pi/4} \frac{1}{2} \ln\left(\frac{T_L}{\tau}\right) d\theta + \int_{\pi/4}^{\tan^{-1}\sqrt{T_L/\tau}} \frac{1}{2} \ln\left(\frac{T_L}{\tau \tan^2\theta}\right) d\theta \\ &= \frac{1}{2} \ln \frac{T_L}{\tau_\eta} \left(\tan^{-1}\sqrt{\frac{\tau_\eta}{\tau}} - \tan^{-1}\sqrt{\frac{\tau_\eta}{T_L}} \right) + \frac{1}{2} \ln \frac{T_L}{\tau} \left(\frac{\pi}{4} - \tan^{-1}\sqrt{\frac{\tau_\eta}{\tau}} \right) + \frac{1}{2} \ln \frac{T_L}{\tau} \left(\tan^{-1}\sqrt{\frac{T_L}{\tau}} - \frac{\pi}{4} \right) \\ &+ \int_{\tan^{-1}\sqrt{\tau_\eta/T_L}}^{\tan^{-1}\sqrt{\tau_\eta/\tau}} \ln(\tan\theta) d\theta - \int_{\pi/4}^{\tan^{-1}\sqrt{T_L/\tau}} \ln(\tan\theta) d\theta \quad I \sim \ln\left(\frac{T_L}{\tau}\right) + \frac{4}{\pi} \int_0^{\pi/4} \ln(\tan\theta) d\theta. \end{aligned} \quad (\text{C6})$$

$$I \sim \ln\left(\frac{T_L}{\tau}\right) + \frac{4}{\pi} \int_0^{\pi/4} \ln(\tan\theta) d\theta. \quad (\text{C7})$$

The variance can be deduced from this calculation:

$$\langle (X_t^\infty)^2 \rangle = \frac{1}{\pi} \int_0^\infty \int_0^\infty \frac{1}{(x+y)\sqrt{xy}} [g_{T_L}(x) - g_{\tau_\eta}(x)] [g_{T_L}(y) - g_{\tau_\eta}(y)] dx dy. \quad (\text{C8})$$

We remark that this expression is similar to the one obtained in Eq. (C2) where τ is replaced by τ_η . Therefore, we obtain

$$\langle (X_t^\infty)^2 \rangle = \ln\left(\frac{T_L}{\tau_\eta}\right) + \frac{8}{\pi} \int_0^{\pi/4} \ln(\tan\theta) d\theta. \quad (\text{C9})$$

-
- [1] J. P. Minier, S. Chibbaro, and S. B. Pope, *Phys. Fluids* **26**, 113303 (2014).
- [2] L. F. Richardson, *Weather Prediction by Numerical Process* (Cambridge University Press, Cambridge, UK, 2007).
- [3] A. N. Kolmogorov, *Cr. Acad. Sci. URSS* **30**, 301 (1941).
- [4] L. D. Landau and E. M. Lifshitz, *Course of Theoretical Physics*, Vol. 3, *Mechanics of Continuous Media* (Nauka, Moscow, 1944).
- [5] A. N. Kolmogorov, *J. Fluid Mech.* **13**, 82 (1962).
- [6] P. K. Yeung and S. B. Pope, *J. Fluid Mech.* **207**, 531 (1989).
- [7] S. B. Pope and Y. L. Chen, *Phys. Fluids A* **2**, 1437 (1990).
- [8] P. K. Yeung, S. B. Pope, A. G. Lamorgese, and D. A. Donzis, *Phys. Fluids* **18**, 065103 (2006).
- [9] B. B. Dubrulle, *J. Fluid Mech.* **867**, P1 (2019).
- [10] M. S. Borgas, *Philos. Trans. R. Soc. London, Ser. A* **342**, 379 (1993).
- [11] U. Frisch and A. N. Kolmogorov, *Turbulence: The Legacy of A. N. Kolmogorov* (Cambridge University Press, Cambridge, UK, 1995).
- [12] K. R. Sreenivasan and R. A. Antonia, *Annu. Rev. Fluid Mech.* **29**, 435 (1997).
- [13] A. M. Yaglom, *Sov. Phys. Dokl.* **11**, 26 (1966).
- [14] L. Seuront, H. Yamazaki, and F. G. Schmitt, in *Marine Turbulence: Theories, Observations, and Models*, edited by H. Z. Baumert, J. Simpson, J. H. Simpson, J. Sundermann, and J. Sundermann (Cambridge University Press, Cambridge, 2005), Chap. 7, pp. 66–78.
- [15] B. B. Mandelbrot, *Multifractals and 1/f Noise* (Springer, New York, 1999), pp. 294–316.
- [16] J. P. Kahane, *Ann. Sci. Math. Québec* **9**, 105 (1985).
- [17] R. Robert and V. Vargas, *Ann. Probab.* **38**, 605 (2010).
- [18] L. Biferale, G. Boffetta, A. Celani, A. Crisanti, and A. Vulpiani, *Phys. Rev. E* **57**, R6261 (1998).
- [19] F. Schmitt and D. Marsan, *Eur. Phys. J. B-Condens. Matter Complex Systems* **20**, 3 (2001).
- [20] J.-F. Muzy and E. Bacry, *Phys. Rev. E* **66**, 056121 (2002).
- [21] L. Chevillard, *Phys. Rev. E* **96**, 033111 (2017).
- [22] R. M. Pereira, L. Moriconi, and L. Chevillard, *J. Fluid Mech.* **839**, 430 (2018).
- [23] L. Goudenège, R. Letournel, and A. Richard, Technical Report (unpublished).
- [24] A. Lanotte, E. Calzavarini, F. Toschi, J. Bec, L. Biferale, and M. Cencini, Heavy particles in turbulent flows RM-2007-GRAD-EULER-2048 (2011), <https://doi.org/10.4121/uuid:607a19d6-32c0-4b33-a8c1-95293637c2ac>.
- [25] L. D. Landau, E. M. Lifshitz, and C. H. Holbrow, *Physics Today* **16**(6), 72 (1963).
- [26] A. S. Monin and A. M. Yaglom, *Statistical Fluid Mechanics. Volume 2. Mechanics of Turbulence* (MIT, Cambridge, UK, 1975).
- [27] W. J. T. Bos and R. Zamansky, *Phys. Rev. Lett.* **122**, 124504 (2019).
- [28] N. Mordant, A. M. Crawford, and E. Bodenschatz, *Physica D* **193**, 245 (2004).

- [29] H. Xu, M. Bourgoïn, N. T. Ouellette, and E. Bodenschatz, *Phys. Rev. Lett.* **96**, 024503 (2006).
- [30] L. Biferale, E. Bodenschatz, M. Cencini, A. S. Lanotte, N. T. Ouellette, F. Toschi, and H. Xu, *Phys. Fluids* **20**, 65103 (2008).
- [31] A. Arnéodo, R. Benzi, J. Berg, L. Biferale, E. Bodenschatz, A. Busse, E. Calzavarini, B. Castaing, M. Cencini, L. Chevillard *et al.*, *Phys. Rev. Lett.* **100**, 254504 (2008).
- [32] N. Mordant, J. Delour, E. Lévêque, A. Arnéodo, and J.-F. Pinton, *Phys. Rev. Lett.* **89**, 254502 (2002).
- [33] B. L. Sawford and P. K. Yeung, *Phys. Fluids* **27**, 65109 (2015).
- [34] L. Chevillard, B. Castaing, A. Arneodo, E. Lévêque, J. F. Pinton, and S. G. Roux, *C. R. Phys.* **13**, 899 (2012).
- [35] P. K. Yeung, S. B. Pope, and B. L. Sawford, *J. Turbul.* **7**, 1 (2006).
- [36] L. Chevillard, R. Robert, and V. Vargas, *Europhys. Lett.* **89**, 54002 (2009).
- [37] L. Chevillard, R. Robert, and V. Vargas, *J. Phys.: Conf. Ser.* **318**, 042002 (2011).
- [38] F. G. Schmitt, *Eur. Phys. J. B* **34**, 85 (2003).
- [39] U. Frisch, P.-L. Sulem, M. Nelkin, B. U. Frisch, P.-L. Sulem, and M. Nelkin, *J. Fluid Mech.* **87**, 719 (1978).
- [40] R. Benzi, G. Paladin, G. Parisi, and A. Vulpiani, *J. Phys. A: Math. Gen.* **17**, 3521 (1984).
- [41] C. Meneveau and K. R. Sreenivasan, *Phys. Rev. Lett.* **59**, 1424 (1987).
- [42] Z. Zhang, D. Legendre, and R. Zamansky, *J. Fluid Mech.* **879**, 554 (2019).
- [43] B. B. Mandelbrot and J. W. Van Ness, *SIAM Rev.* **10**, 422 (1968).
- [44] P. Carmona and L. Coutin, *Electron. Commun. Probab.* **3**, 95 (1998).
- [45] P. Harms, *Discr. Contin. Dynam. Syst. B* **26**, 5567 (2021).